Full Paper
Journal of Nano Materials Impact 2025, 01 (02) 24-32

Simulation and Application of Practical Data of the Nano Ablation of Cancerous Tumors Using Laser Knife

Baneen Salim Abd[1], Bahjat B. Kadhim[*, 2], Mariam Mohamed Abud[1]
[1]Department of Physics, College of Education, Mustansiriyah University, IRAQ. [2]Department of Physics, College of Science, Mustansiriyah University, IRAQ.

Abstract
A simulation of nano ablating an induced cancerous tumor in the thigh of a sheep was conducted after slaughtering it. The simulation was conducted on the assumption that the tumor and cancer occurred due to the abnormal growth of one of the amino acids that make up the collagen protein, which is proline, with a percentage of cancer cell division ranging from 10% to 90% in the tissues of the thigh of the sheep, as collagen is one of the proteins that make up the connective tissue of the thigh of the sheep. The surgical ablation of the aforementioned cancer was carried out practically using a laser knife, by implementing the output data obtained from the computational simulation. The Gauss View 6.0.16 program was used to build the spatial structure of the collagen protein and the amino acid proline, and the Gaussian 09 program was used to simulate the physical properties. A simulation program written in Fortran 90 was used to calculate the rate and time of tumor ablation, using the finite difference method, by using the data obtained from the simulation of physical properties by the Gaussian 09 program. A CO2 laser knife with a wavelength of 10600 nm was used to perform the tumor ablation operation. The simulation was carried out using the density functional theory method at the B3LYP level, in conjunction with the 6 – 311G(d,p) basis set. There was a great match between the rate of ablation in the simulation and the rate of ablation in the practical, as they were (1.87) mm/sec and (2.25) mm/sec, for 90 Vol. % respectively. It can be concluded from the results of the study that the simulation data can be used to help represent a surgical ablation operation with high accuracy in terms of time and rate of ablation.

Keyword: collagen • proline • ablation • laser knife • gaussian • induced cancerous tumor • DFT.

Introduction

Materials science is an interdisciplinary field that studies material properties and their applications in science and engineering. This science explores how materials' structure affects their properties. It combines applied physics and chemistry, as well as chemical, mechanical, and electrical engineering. Recently, advances in nanoscience and nanotechnology have elevated materials science to a new level[1]. Despite 80 years of dedicated drug discovery research, cancer remains the leading cause of death worldwide[2]. Efforts to eradicate cancer have been hindered by numerous challenges in treatment and diagnosis.

Cancer therapeutics face a significant challenge due to the diverse genetic alterations found in each type of cancer. Tumor heterogeneity leads to resistance to single-target drug approaches, necessitating the use of combination therapies[3, 4].

***Address for correspondence:** Prof. Dr. Bahjat B. Kadhim, Department of Physics, College of Science, Mustansiriyah University, Baghdad 10052, Iraq.
E-mail: sci.phy.bbk@uomustansiriyah.edu.iq
ORCID: https://orcid.org/0000-0001-9964-8226

Info:
Submitted: 07 Nov. 2024; **Revised:** 02 May 2025;
Accepted: 15 June 2025; **Published:** 18 Aug. 2025.
https://doi.org/10.71109/nmi.2025.1.2.9

There has been a great development in all sciences due to the development of computers and computing, as it has become possible to simulate or model different and multiple systems through advanced programs quickly and permanently. The field of medicine has achieved great and tremendous development in terms of the use of various, accurate, and advanced treatments, or through devices and equipment used in diagnosis or treatment. Among the most important diseases that threaten humanity is cancer in all its types. From time to time, we see the emergence of a new and advanced technology or method that deals with cancer. Among the developments that have occurred in surgical operations to remove cancerous tumors is the use of laser devices instead of traditional scalpels that cause a long period of time for wounds to heal, and may cause infections that burden the patient with an additional burden in the long period of treatment compared to the use of laser scalpels called laser knives[5-7].

Several types of lasers are currently being used in maxillofacial surgery. Laser beams affect biological tissue based on their wavelength, which can be reflected, scattered, or absorbed[8]. Tissues are composed of diverse components that can differ between types and within the tissue structure. The optical properties of a tissue are influenced by its component substances, as well as their concentration and distribution. Water, hemoglobin, and melanin are the most studied components of biological tissue for their impact on light in the UV-IR spectrum. Recent research has focused on the roles of collagen, hydroxyapatites, and lipids. When selecting a laser, clinicians should choose a wavelength that is most efficiently absorbed by the target tissue or compound[9]. In order to increase the reliability of using the laser knife in surgical operations, a simulation is performed

by implementing simulation programs that are built according to the required surgical operations. Among the most important programs used in the simulation and modeling of different systems and materials are Gaussian, CASTEP, SIESTA, Monte Carlo, and others[10]. This is in addition to building special simulation programs, and according to the case to be studied, the above programs support and are implemented for the data obtained from them. In these cases, multiple and different languages are used in building simulation programs. The finite difference method and the finite element difference method that use Fortran language are considered the most important methods in building simulation programs[11]. In our current study, the finite difference method was used in Fortran 90 language to build a cancer tumor ablation simulation program based on the Gaussian 09 program to obtain the physical data required to feed the finite difference simulation program, which was built according to the experimental data of the surgical ablation of a sheep thigh infected with cancer induced in the connective tissue, specifically in one of the proteins that make up the tissue, and in one of the amino acids that make up the collagen protein (There are 19 total amino acids in collagen (8 of which are essential): Alanine, Arginine, Asparagine, Aspartate, Cysteine, Glutamate, Glutamine, Glycine, Histidine, Isoleucine, Leucine, Lysine, Methionine, Phenylalanine, Proline, Serine, Threonine, Tyrosine, and Valine), while the amino acid was proline [$C_5H_9NO_2$]. The connective tissue of a sheep thigh consists of a group of proteins including; Elastin 10%, Dermatan Sulfate 30%, Heparan Sulfate 5%, Collagen 40%, Chonderoitin, sulfate 5%, Keratin 5% and Reticulin 5%[12].

Many studies have been conducted on the subject of using laser scalpels practically in ablating cancerous tumors in different places in the human body, especially those cancers that are in places that are difficult to deal with surgically with traditional scalpels[13]. The current study aims to implement a physical simulation of a surgical ablation of a type of cancerous tumor induced in the thigh of a sheep, by employing the Gaussian 9 simulation program in conjunction with the Gauss View 6 program, to assist specialist doctors in dealing with the laser knife and increase the reliability and accuracy of the surgical ablation process.

Experimental Part

Theoretical Considerations

Several studies have shown that thermal ablation techniques are clinically effective for treating tumors; several thermal ablation techniques are currently available in clinical settings[14]. Thermal ablation (TA) is becoming increasingly popular for treating small and mid-sized tumors. Miniature percutaneous or endoscopic applicators heat the surrounding tissue with high selectivity, causing cell damage in a targeted area around the tumor[15]. The goal of hyperthermic ablative procedures is to cause direct cellular injury through the application of heat. This occurs after 1-2 minutes at 50°C and within seconds above 60°C[16]. The CO_2 laser causes soft tissue damage in three zones: an outer layer of carbonized material, a zone of vacuolation (cavities formed by the explosive conversion of water to steam), and a coagulated zone (formed at temperatures below 100 °C)[17]. When photons are well absorbed and concentrated in a small volume, tissue temperature rises significantly compared to when photons are poorly absorbed and spread out over a larger area. To efficiently and effectively reach the vaporization threshold, use a wavelength that the target tissue can absorb. Water is the most commonly targeted tissue component for beam absorption in soft tissue cutting and ablative applications due to its difficulty in reaching the ablation threshold and causing subablative thermal injury. The Er:YAG and CO_2 laser wavelengths exhibit high water absorption coefficients[18, 19].

The Fourier-conduction-based Penne bioheat transfer equation is the most commonly used model for analyzing heat transfer in biological tissues during thermal ablative procedures due to its simplicity and feasibility[20].

$$\rho C\frac{\partial T}{\partial t} = \nabla(k\nabla T) + \rho_b C_b \omega_b (T_b - T) + Q_{met} + Q_{laser} - Q_{vap} \quad \ldots (1)$$

where T is the temperature at which blood enters the tissue, ρ_b is the density of blood (kg/m^3), C_b is the specific heat capacity of blood (J/kg.K), ω_b is the blood perfusion rate (1/s), T_b is the temperature of blood entering the tissue, and the term [ρ_b C_b ω_b (T_b-T)] simulates the tiny capillary vasculature's heat-sink effect, Q_{vap} (W/m^3) is the heat generation (or source term) during thermal ablative procedures and is highly dependent on the type of therapy under consideration, Q_{met} (W/m^3) is the heat generated by metabolism, which is typically ignored due to its minimal impact compared to other heat sources and external heat source Q_{laser}, the term that is dependent on time is indicated on the left side of equation (1) first thing.

The thermal properties of materials are closely related to heat capacity, primarily through lattice vibrations in insulators and conduction electrons in metals, with additional aspects such as thermal expansion and conductivity (K) [20], The thermal conductivity (K) of a substance is defined as the amount of heat (Q) transmitted by a unit temperature gradient in a direction normal to a surface of unit area in unit time under steady-state conditions. Heat transfer is solely dependent on the temperature gradient[21]:

$$\frac{Q}{A} = -K\frac{\partial T}{\partial X} \quad \ldots (2)$$

In this equation, $\partial T/\partial X$ represents the temperature gradient in the heat flow direction, and A represents the cross-sectional area. The negative sign indicates that the heat flux is causing the temperature to decrease.

When steady-state conditions are not applicable, thermal diffusivity (α) in (Ws^{½}/m^2.K) is used[22]:

$$\alpha = \frac{K}{\rho C_V} \quad \ldots (3)$$

where C_V is the specific heat capacity and ρ is the density. α is related to the spatial and temporal variation of temperature (T) in the medium by[23]:

$$\frac{\partial T}{\partial t} = \alpha\nabla^2 T \quad \ldots (4)$$

The value of α represents the rate at which temperature changes over time.

Thermal resistance in most materials is calculated by dividing the temperature difference by the heat flux (q). This method was applied to evaporator wick, nanoscale thin films, and nanofluid in a tube. Therefore, the thermal resistance can be expressed as[24]:

$$R = \frac{\Delta X}{K} = \frac{-\Delta T}{q} \quad \text{... (5)}$$

R represents thermal resistance, ΔX is the thickness between inside and outside tissues, and ΔT is the temperature difference between the two. Mathematical modeling has been widely used to improve the efficacy of thermal ablative therapies and provide a priori estimates of treatment outcomes during the planning stage. Numerical modeling and simulations can effectively predict tissue response to thermotherapies. The predictions are based on two major mathematical models: bioheat transfer and tissue damage. This section outlines the framework for various therapeutic models used in clinical practice[25].

The finite difference method relies on different approximations to be substituted into partial differential equations. For instance, the heat transfer equation in rectangular coordinates is given by[26]:

$$\frac{\partial T}{\partial t} = \left(\frac{K}{\rho C_V}\right)\left(\frac{\partial^2 T}{\partial x^2} + \frac{\partial^2 T}{\partial y^2} + \frac{\partial^2 T}{\partial z^2}\right) + Q \quad \text{... (6)}$$

The ablation rate (A_r) represents the material's mass loss rate and is equal to the ratio of ablation amount to ablation time[27]:

$$A_r = \frac{\Delta d}{t} \quad \text{... (7)}$$

where Δd is the ablation thickness (mm), and t is the working time (sec).

The periodontium is a distinct anatomical site with four connective tissues: gingiva, periodontal ligament, cementum, and alveolar bone. Connective tissues are typically divided into fibrous and non-fibrous elements. Collagens and proteoglycans are well-studied components that play a significant role in skeletal and soft connective tissues. Collagen accounts for approximately 40% of total protein in the human body[28]. Collagen is classified into seven broad classes, with approximately 27 recognized types. Fibrillar collagen, specifically types I, III, and VI, is a major component of connective tissue. Oral mucosa's anchoring fibrils are composed of collagen type VII. The distinguishing feature is a unique triple helix with unusual cross-links[29]. Tropocollagen is a left-handed, α-helix molecule with three spirally wound polypeptide chains **Figure 1**. Tropocollagen molecules aggregate through electrostatic and hydrophobic side bonds, forming collagen fibers. Aggregation leads to cross-links, including covalent and non-covalent bonds between fibrils. The amino acids lysine (Lys-Lys) and hydroxyproline (Hyl-Hyl) form a pair[30, 31].

Materials and Methodology

To ablate all the thigh of a sheep tissues, it was heated to 100 ˚C, which causes the tissue to vaporize. Our goal was to model tissue ablation while minimizing thermal injury, as proteins of a sheep thigh at temperatures above 60ºC, the tissues are considered damaged after that point[32].

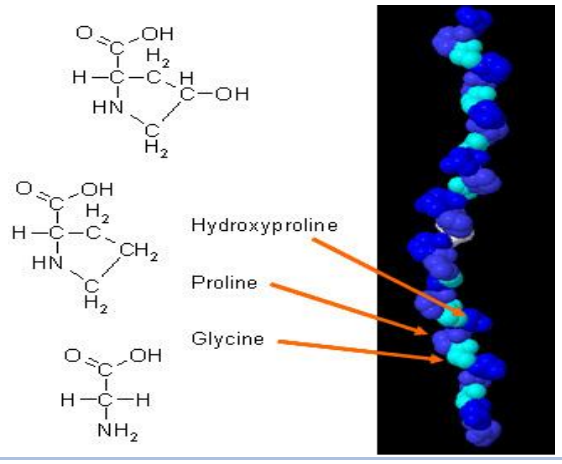

Figure 1. High-resolution crystal structure of a collagen triple helix, formed from (ProHypGly)–(ProHypAla)–(ProHypGly) [30, 31].

The sheep thigh tissue's extracellular matrix contains both fibrous and nonfibrous elements such as collagens, elastin, fibronectin, laminin, osteopontin, bone sialoprotein, growth factors, proteoglycans, lipids, minerals, and water[33]. The interactions between these components affect tissue health, damage, repair, and regeneration[34]. The study assumes that the occurrence of cancer in the sheep thigh tissue. Collagen protein was chosen as the tissue where an imbalance will occur that leads to cancer. Collagen is the primary component of the connective tissue extracellular matrix. Collagen protein contains the amino acids hydroxyproline, glycine, and proline. The study assumes that one of these amino acids, Proline, undergoes multiple divisions in the Collagen protein, resulting in cancer[35, 36].

The ablation of cancer in the sheep thigh tissue area was simulated using a tumor ablation program with a laser knife. The physical and thermodynamic properties of the sheep thigh tissue components were obtained using the online Gaussian 09 program by employing Gauss View 6.0.16. The Gaussian 09 program has been used to implement simulations. The Gaussian 09 program is based on calculating the total energy of the system by applying the Schrödinger equation to the system's particles based on a basis set and system-specific functions.

The Gaussian 09 program can simulate the sheep thigh tissue under consideration, calculating its structural and thermal properties. Density functional theory (DFT) is a key method for calculating the electronic structure of solids, molecules, and atoms. The standard 6-311G(d,p) basis set was used for all models at the B3LYP level when using density functional theory (DFT)[37]. Using an internally developed finite difference method (FDM) with the FORTRAN 90 language. The finite difference method (FDM) was used as a technique to solve the thermal problem under appropriate boundaries. The 3-D domain is used in conjunction with a multilevel blood vessel-infused tumor and a modified 3-D triple-layered structure to directly determine the temperature and thermal deformation history in terms of thermal properties[38].

Results and Discussion

Through the Gaussian 09 program coupled with Gauss View

6.0.16, the optimal structure of all components of the sheep thigh tissue was obtained, as shown in **Figure 2**. The physical properties of density, specific heat, and thermal conductivity were obtained to implement the simulation of the assumed tumor ablation process according to the study of the sheep thigh tissue ablation using a laser knife. Also, Figure 2 describes the structure of the amino acid Proline, which will be the main pathogenic cause of cancer in Collagen.

Through the results of the optimal structural properties of the proteins of the connective tissue components of the sheep thigh under the simulation study, and then obtaining the physical data, which were used in the simulation program for the surgical ablation of the area affected by cancer in the sheep thigh, and when comparing the composition of the optimal structure of the proteins that make up the connective tissue with the optimal structure available in many studies[39], it can be noticed the great and ideal match in the composition of the optimal structures, and this can be explained by understanding the mechanism of the implemented simulation program, represented by the Gaussian 09 program, where the simulation implementation processes are carried out by using the density functional theory in solving the Schrödinger equation to obtain the total energy of the optimal structure at the lowest energy, and the period of running the program ranged between several minutes and several hours, during which the simulation program works to change the values of the bond lengths and the values of the tetrahedral angles and the values of the dihedral angles over the time of running and executing the program, until the optimal structure is obtained. The agreement between the optimal structures obtained from the simulation and the optimal structures available in the scientific literature indicates that the use of the B3LYP approximation compatible with the basis set 6 – 311G(d,p) was correct, accurate, and ideal. The difference in the average value of the bond length did not exceed (0.001) Angstroms[40, 41].

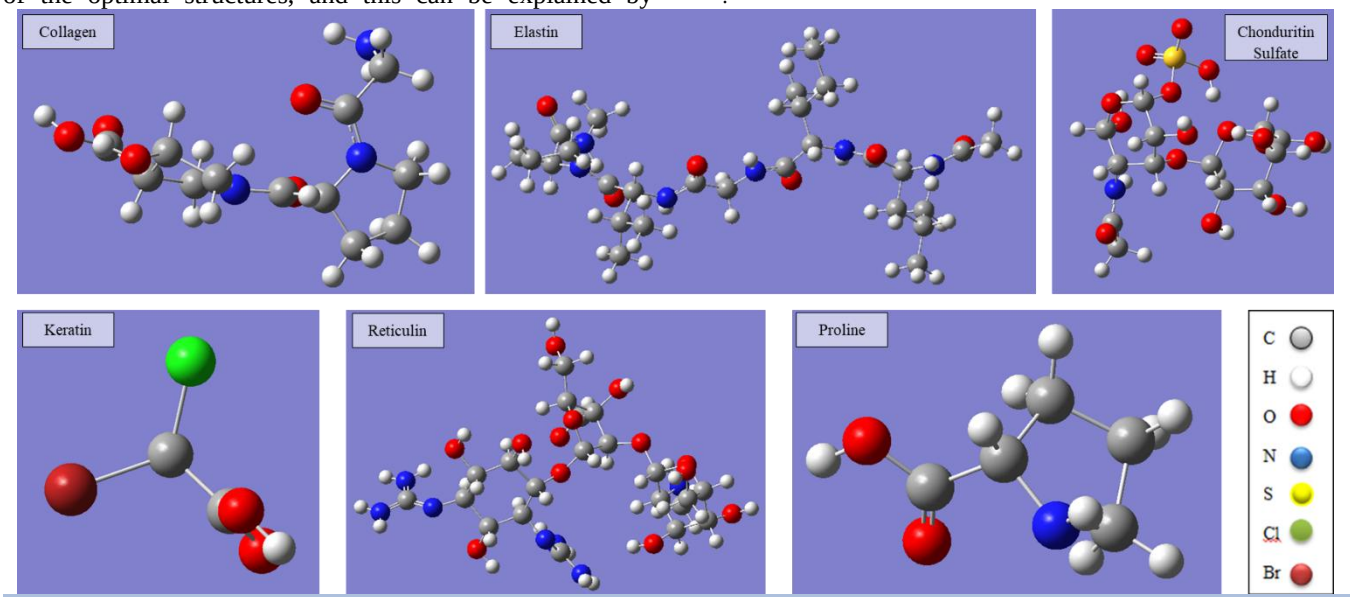

Figure 2. Optimal structure of all components of the sheep thigh tissue.

Table 1 describes the physical properties that will be used to simulate the ablation process using a laser knife. Through the results in Table 1, represented by the total energy, thermal conductivity, specific heat, and density of each of the proteins in the sheep thigh tissue components, in addition to the amino acid Proline, which causes the multiple divisions of the sheep thigh tissue cancer. A simulation of the ablation process of the cancer under study was carried out, with volume ratios of the causative agent Proline ranging from (10 - 90) Vol. % with a fixed increase rate of 10 Vol.%.

Table 1. Total energy SCF, density ρ, specific heat C_V, and thermal conductivity λ of the sheep thigh tissue.

Tissue	SCF (eV)	λ (W/mK)	$(\lambda)_T$ (W/mK)	P (Kg /m^3)	$(\rho)_T$ (Kg /m^3)	C_V (J /Kg. K)	$(C_V)_T$ (J /Kg. K)
Elastin 10%	-50028.08	0.04		126.65		1225.93	
Dermatan Sulfate 30%	-57938.81	0.03		1549.90		1036.29	
Heparan Sulfate 5%	-57574.87	0.03		2715.20		765.66	
Collagen 40%	-27466.58	0.09	**0.052**	1439.70	**1447**	1075.03	**1025**
Chondroitin sulfate 5%	-56869.18	0.03		1549.90		1015.47	
Keratin 5%	-88774.16	0.01		2251.40		503.24	
Reticulin 5%	-59468.37	0.02		1353.20		949.32	
Proline	-10913.93	0.752	**0.752**	1255.84	**1255.84**	991.79	**991.79**

Table 2 describes the simulation results, where the ablation rate and the time rate of the ablation process were obtained according to the volumetric ratios, in addition to the thermal diffusivity and effusivity properties, which helped in understanding and discussing the simulation of the ablation process. The results of the simulation of the ablation process for healthy tissue and for volume ratios of (10 - 90) Vol.% in **Figures 3 – Figure12** were chosen only because they are sufficient for this, which represents the temperature distribution after a few seconds when the sheep thigh tissue

of Vol.% Proline pathogenic cancer is ablated by simulation operation of Laser knife temperature for side and top view.

Table 2. Ablation rate simulation results.

Vol.% of cancer	Time (sec)	Ablation rate (mm/sec)	Thermal effusivity ($Ws^{½}/m^2.K$)	Thermal diffusivity (m^2/s)
0	17.89	3.35E-001	3.50E-008	277.678
10	17.04	3.52E-001	6.16E-008	362.089
20	15.97	3.75E-001	8.95E-008	429.324
30	14.71	4.08E-001	1.19E-007	486.964
40	13.25	4.53E-001	1.51E-007	538.709
50	11.59	5.17E-001	1.85E-007	587.116
60	9.74	6.15E-001	2.24E-007	634.779
70	7.72	7.77E-001	2.71E-007	685.791
80	5.53	1.08	3.37E-007	750.263
90	3.21	1.87	4.72E-007	872.236

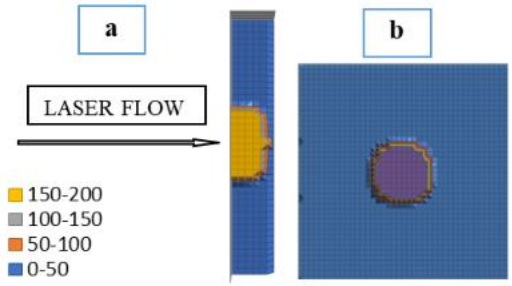

Figure 3. Temperature distribution in ^oC after 17.895 seconds when 0 Vol.% Proline pathogenic cancer of the gingival tissue is ablated by the simulation operation of laser knife temperature. (a) side view, (b) top view.

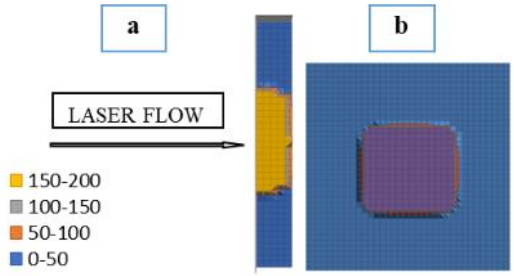

Figure 4. Temperature distribution after 17.04 seconds when 10 Vol.% Proline pathogenic cancer of the gingival tissue is ablated by the simulation operation of laser knife temperature. (a) side view, (b) top view.

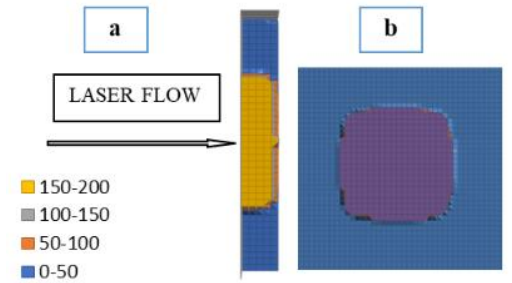

Figure 5. Temperature distribution in ^oC after 15.975 seconds when 20 Vol.% Proline pathogenic cancer of the gingival tissue is ablated by the simulation operation of laser knife temperature. (a) side view, (b) top view.

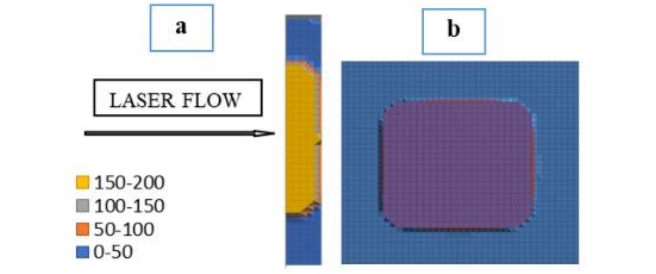

Figure 6. Temperature distribution in ^oC after 14.71 seconds when 30 Vol.% Proline pathogenic cancer of the gingival tissue is ablated by the simulation operation of laser knife temperature. (a) side view, (b) top view.

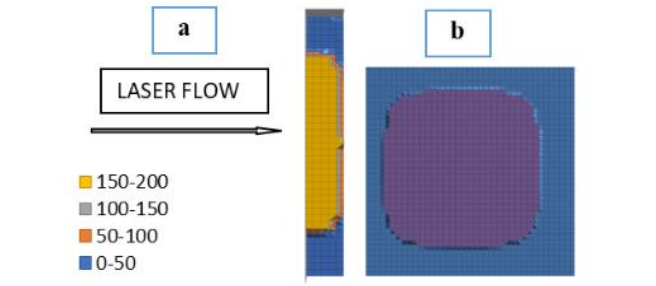

Figure 7. Temperature distribution in ^oC after 13.25 seconds when 40 Vol.% Proline pathogenic cancer of the gingival tissue is ablated by the simulation operation of laser knife temperature. (a) side view, (b) top view.

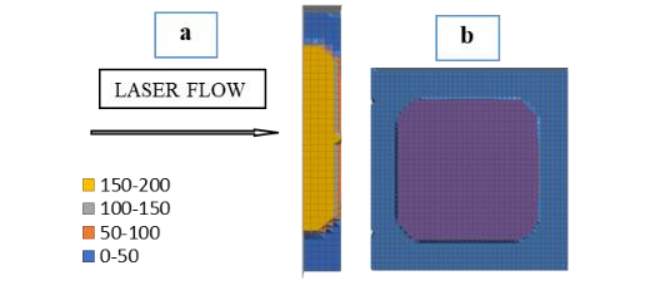

Figure 8. Temperature distribution in ^oC after 11.59 seconds when 50 Vol.% Proline pathogenic cancer of the gingival tissue is ablated by the simulation operation of laser knife temperature. (a) side view, (b) top view.

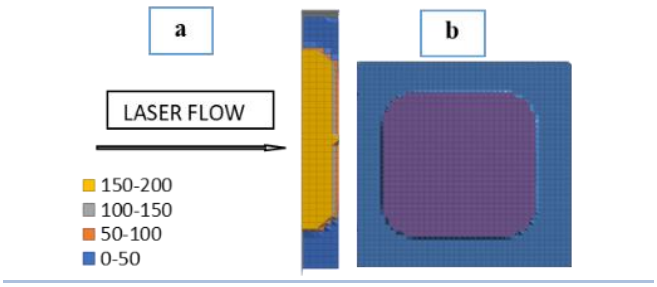

Figure 9. Temperature distribution in ^oC after 9.745 seconds when 60 Vol.% Proline pathogenic cancer of the gingival tissue is ablated by the simulation operation of laser knife temperature. (a) side view, (b) top view.

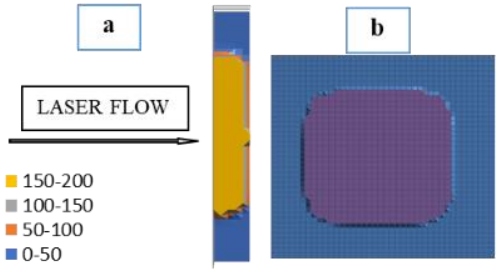

Figure 10. Temperature distribution in ^{o}C after 7.72 seconds when 70 Vol.% Proline pathogenic cancer of the gingival tissue is ablated by the simulation operation of laser knife temperature. (a) side view, (b) top view.

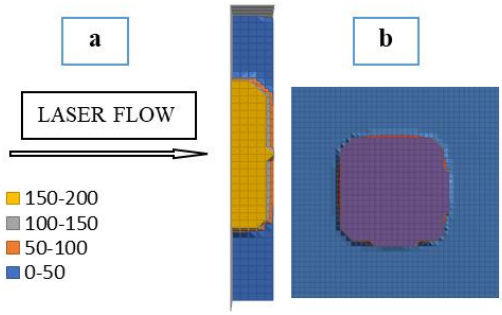

Figure 11. Temperature distribution in ^{o}C after 5.53 seconds when 80 Vol.% Proline pathogenic cancer of the sheep thigh tissue is ablated by the simulation operation of laser knife temperature. (a) side view, (b) top view.

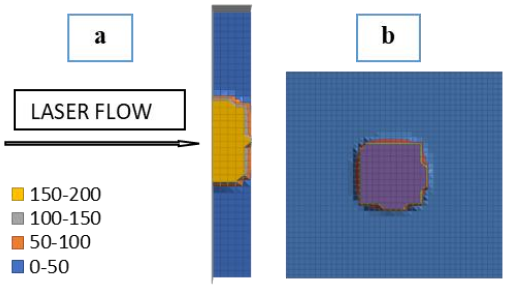

Figure 12. Temperature distribution in ^{o}C after 3.21 seconds when 90 Vol.% Proline pathogenic cancer of the sheep thigh tissue is ablated by the simulation operation of laser knife temperature. (a) side view, (b) top view.

The results of **Table 2** can be explained as follows: the cancer cell death is the primary goal of all cancer treatments. Photo thermal therapy (PTT) is a highly effective form of thermal therapy that kills cancer cells by exposing them to high-temperature radiation above 40°C. PTT causes tumor death by converting light to heat when photo-absorbers are exposed to a near-infrared (NIR) laser. PTT can be used locally to treat cancer cells in primary tumors or metastases[42]. Understanding laser light fundamentals is crucial for understanding its applications in surgery. Lasers outperform other light sources in terms of power, beam quality, and coherence. Lasers emit coherent, monochromatic, and collimated electromagnetic radiation with high intensity, resulting in higher optical power per unit area for a given amount of energy than broadband light sources. These characteristics give the laser a unique set of applications. Each type of laser has unique features, such as spot size, wavelength, and radiance[43]. Laser energy can disrupt tissue through photo-thermal, photo-ablative, photo-disruptive, or photochemical mechanisms. Most surgical laser systems primarily affect tissue through photothermal effects. Photons are absorbed in tissue, converted to thermal energy, and alter the tissue due to the thermal change[9]. High-power pulsed lasers offer accurate tissue incision with minimal thermal damage to surrounding healthy tissue, making them a valuable tool in surgery. Pulsed CO_2 lasers are widely used for precise cutting, minimal thermal damage, and simultaneous hemostasis of small vessels[44]. The ablation results seen in Figures 3 – Figure 12 can be explained by assuming that the three-dimensional propagation of the temperature front acts as a gauge for tissue ablation[45]. In accordance with Platnick et.al., the simulation technique may replicate the extensive thermal damage resulting from laser-induced ablation of actual tissues by incorporating density, specific heat, and thermal conductivity characteristics for the thermal ablation of tissue proteins. This new surgical technique, called superficial and a real ablation, uses a laser to ablate precancerous growths from specific parts of the sheep thigh tissue[46].

The basic theory of ablation could be used to discuss the results of cancerous ablative; that is, the thermal flux applied to the front of the materials under ablation acts as a heat sink. Then, as the heat is applied, the first layers of materials become viscous and eventually reach the degraded case, producing either char or volatilization, which causes the material to decompose[47].

The laser spot is thought to be circular and follows a small heat source. The spot size and cross-section of a laser are the same thing. The fluency and irradiance of a laser beam are directly affected by the spot size; the square of the spot size radius is inversely proportional to both flux and irradiance, so a four-fold increase in the energy or power density occurs when the spot size is halved. A smaller spot size allows for more scattering to occur sideways and backwards, which causes the tissue's energy fluency to decrease more quickly than it would with a larger spot size. A large spot size is necessary for maximum laser light penetration in order to reach deeper or mid-dermal targets[48]. At spot sizes, a rise in penetration depth levels out. The length of time the individual is exposed to the laser beam determines how quickly the energy is supplied.

Finally, here was a great match between the rate of ablation in the simulation and the rate of ablation in the practical, as they were (1.87) mm/sec and (2.25) mm/sec, for 90 Vol. % respectively.

Conclusion

It can be inferred from the simulation results using the Gaussian program that the program can be used to obtain thermal properties like specific heat and thermal conductivity, which are crucial parameters in the program to ablate cancer tumors, as well as physical properties represented by density. According to the simulation results of the ablation process, which are represented by the time and rate of ablation, it is possible to substitute a laser knife for standard metal surgical scalpels in order to ablate a cancerous tumor in the tissue of the sheep's thighs. This procedure offers

accuracy and faster healing than standard surgical procedures.

Acknowledgements

The authors would like to acknowledge Department of Physics, College of Sciences, Mustansiriyah University, Baghdad, Iraq.

Declaration of Competing Interests

The authors declare that they have no conflicts of interest.

References

[1] H.-J. Fecht, "Materials Science," in *Generation and applications of extra-terrestrial environments on earth*, D. A. Beysens and J. J. Van Loon, Eds. 1 ed.: Taylor & Francis, 2015, pp. 211-218.

https://doi.org/10.1201/9781003338277-26.

[2] V. T. DeVita, Jr. and E. Chu, "A History of Cancer Chemotherapy," *Cancer Research*, vol. 68, no. 21, p. 8643-8653, 2008.

https://doi.org/10.1158/0008-5472.CAN-07-6611.

[3] T. A. Denison and Y. H. Bae, "Tumor heterogeneity and its implication for drug delivery," *Journal of Controlled Release*, vol. 164, no. 2, p. 187-191, 2012.

https://doi.org/10.1016/j.jconrel.2012.04.014.

[4] I. Dagogo-Jack and A. T. Shaw, "Tumour heterogeneity and resistance to cancer therapies," *Nature Reviews Clinical Oncology*, vol. 15, no. 2, p. 81-94, 2018.

https://doi.org/10.1038/nrclinonc.2017.166.

[5] A. Jemal, F. Bray, M. M. Center, J. Ferlay, E. Ward, and D. Forman, "Global cancer statistics," *CA: A Cancer Journal for Clinicians*, vol. 61, no. 2, p. 69-90, 2011.

https://doi.org/10.3322/caac.20107.

[6] C. R. Leemans, P. J. F. Snijders, and R. H. Brakenhoff, "The molecular landscape of head and neck cancer," *Nature Reviews Cancer*, vol. 18, no. 5, p. 269-282, 2018.

https://doi.org/10.1038/nrc.2018.11.

[7] J. Ferlay *et al.*, "Cancer statistics for the year 2020: An overview," *International Journal of Cancer*, vol. 149, no. 4, p. 778-789, 2021.

https://doi.org/10.1002/ijc.33588.

[8] F. W. Neukam and F. Stelzle, "Laser tumor treatment in oral and maxillofacial surgery," *Physics Procedia*, vol. 5, p. 91-100, 2010.

https://doi.org/10.1016/j.phpro.2010.08.125.

[9] G. M. Peavy, "Lasers and laser–tissue interaction," *Veterinary Clinics of North America: Small Animal Practice*, vol. 32, no. 3, p. 517-534, 2002.

https://doi.org/10.1016/S0195-5616(02)00003-7.

[10] E. Darrigues, Z. A. Nima, R. J. Griffin, J. M. Anderson, A. S. Biris, and A. Rodriguez, "3D cultures for modeling nanomaterial-based photothermal therapy," *Nanoscale Horizons*, 10.1039/C9NH00628A vol. 5, no. 3, p. 400-430, 2020.

https://doi.org/10.1039/C9NH00628A.

[11] D. Gabrić *et al.*, "Application of Diode Laser in Oral and Maxillofacial Surgery," in *A Textbook of Advanced Oral and Maxillofacial Surgery*, M. H. K. Motamedi, Ed. Rijeka: IntechOpen, 2013.

https://doi.org/10.5772/52404.

[12] E. N. Sobol, M. Makropoulou, A. A. Serafetinides, and D. Yova, "Theoretical model of CO_2 laser ablation of soft-tissue phantoms," *Il Nuovo Cimento D*, vol. 18, no. 4, p. 483-490, 1996.

https://doi.org/10.1007/BF02451812.

[13] S. Zhang *et al.*, "Modeling and ex vivo experimental validation of liver tissue carbonization with laser ablation," *Computer Methods and Programs in Biomedicine*, vol. 217, p. 106697, 2022.

https://doi.org/10.1016/j.cmpb.2022.106697.

[14] Y. Liu *et al.*, "Characterization of tumour laser ablation probes with temperature measuring capabilities," in *2015 International Conference on BioPhotonics (BioPhotonics)*, 2015, pp. 1-4.

https://doi.org/10.1109/BioPhotonics.2015.7304016.

[15] S. Singh and R. Melnik, "Thermal ablation of biological tissues in disease treatment: A review of computational models and future directions," *Electromagnetic Biology and Medicine*, vol. 39, no. 2, p. 49-88, 2020.

https://doi.org/10.1080/15368378.2020.1741383.

[16] F. Partovi *et al.*, "A model for thermal ablation of biological tissue using laser radiation," *Lasers in Surgery and Medicine*, vol. 7, no. 2, p. 141-154, 1987.

https://doi.org/10.1002/lsm.1900070202.

[17] O. T. Farouki, "The thermal properties of soils in cold regions," *Cold Regions Science and Technology*, vol. 5, no. 1, p. 67-75, 1981.

https://doi.org/10.1016/0165-232X(81)90041-0.

[18] K. Giering, O. Minet, I. Lamprecht, and G. Müller, "Review of thermal properties of biological tissues," in *Laser-induced interstitial thermotherapy*, Berlin, Germany, 1995, pp. 45-65: SPIE, Bellingham WA.

[19] A. M. Hassan and A. A. Muhmood, "Nonlinear Optical Properties of Core@Shell Nanoparticles of Gold and Moringa Oleifera Leaves via Laser Ablation Technique," *Journal of Nano Materials Impact*, vol. 1, no. 1, p. 19-24, 2025.

https://doi.org/10.71109/nmi.2025.1.1.7.

[20] L. Wang, D. Chong, Y. Di, and H. Yi, "A revised method to predict skin's thermal resistance," *Thermal Science*, vol. 22, no. 4, p. 1795-1802, 2018.

https://doi.org/10.2298/TSCI1804795W.

[21] K. Zhang, C. Wang, Q. Li, and Z. Wang, "Characterization of the Nozzle Ablation Rate Based on 3D Laser Scanning System," *Aerospace*, vol. 10, no. 2,

https://doi.org/10.3390/aerospace10020172

[22] A. L. McKenzie, "A three-zone model of soft-tissue damage by a CO_2 laser," *Physics in Medicine & Biology*, vol. 31, no. 9, p. 967, 1986.

https://doi.org/10.1088/0031-9155/31/9/003.

[23] I. R. David and A. P. Leslie, "Modeling Of The Laser-Induced Ablation And Thermal Damage Of Biological Tissue," in *Proc.SPIE*, 1989, vol. 1064, pp. 30-39.

https://doi.org/10.1117/12.951944.

[24] P. M. Bartold, "Connective tissues of the periodontium. Research and clinical implications," *Australian Dental Journal*, vol. 36, no. 4, p. 255-268, 1991.

https://doi.org/10.1111/j.1834-7819.1991.tb00720.x.

[25] P. Rajalalitha and S. Vali, "Molecular pathogenesis of oral submucous fibrosis – a collagen metabolic disorder," *Journal of Oral Pathology & Medicine*, vol. 34, no. 6, p. 321-328, 2005.

https://doi.org/10.1111/j.1600-0714.2005.00325.x.

[26] M. D. Shoulders and R. T. Raines, "Collagen Structure and Stability," *Annual Review of Biochemistry*, vol. 78, no. Volume 78, 2009, p. 929-958, 2009.

https://doi.org/10.1146/annurev.biochem.77.032207.120833.

[27] A. Owczarzy, R. Kurasiński, K. Kulig, W. Rogóż, A. Szkudlarek, and M. Maciążek-Jurczyk, "Collagen - structure, properties and application," *Engineering of Biomaterials*, no. 156, p. 17-23, 2020.

https://doi.org/10.34821/eng.biomat.156.2020.17-23.

[28] R. Bender, M. Gross, W. Luo, and E. Tess, "Thermal Modeling of Tissue Ablation During Pulsed CO_2 Laser Gingivectomy for Gum Reshaping and Reduction," Cornell University2014.

[29] H. E. Schroeder and M. A. Listgarten, "The gingival tissues: the architecture of periodontal protection," *Periodontology 2000*, vol. 13, no. 1, p. 91-120, 1997.

https://doi.org/10.1111/j.1600-0757.1997.tb00097.x.

[30] N. Buduneli, *Biomarkers in Periodontal Health and Disease: Rationale, Benefits, and Future Directions*. Springer Cham, 2020.

https://doi.org/10.1007/978-3-030-37317-7.

[31] A. Daolio *et al.*, "Molecular electrostatic potential and noncovalent interactions in derivatives of group 8 elements," *Angewandte Chemie*, vol. 133, no. 38, p. 20891-20895, 2021.

https://doi.org/10.1002/ange.202107978.

[32] P. Politzer and J. S. Murray, "Molecular Electrostatic Potentials: Significance and Applications," in *Chemical Reactivity in Confined Systems*, 2021, pp. 113-134.

https://doi.org/10.1002/9781119683353.ch7.

[33] A. Higuchi, Q.-D. Ling, S.-T. Hsu, and A. Umezawa, "Biomimetic Cell Culture Proteins as Extracellular Matrices for Stem Cell Differentiation," *Chemical Reviews*, vol. 112, no. 8, p. 4507-4540, 2012.

https://doi.org/10.1021/cr3000169.

[34] S. A. Eming, M. Hammerschmidt, T. Krieg, and A. Roers, "Interrelation of immunity and tissue repair or regeneration," *Seminars in Cell & Developmental Biology*, vol. 20, no. 5, p. 517-527, 2009.

https://doi.org/10.1016/j.semcdb.2009.04.009.

[35] M. KjÆR, "Role of Extracellular Matrix in Adaptation of Tendon and Skeletal Muscle to Mechanical Loading," *Physiological Reviews*, vol. 84, no. 2, p. 649-698, 2004.

https://doi.org/10.1152/physrev.00031.2003.

[36] E. J. Kay, G. Koulouras, and S. Zanivan, "Regulation of Extracellular Matrix Production in Activated Fibroblasts: Roles of Amino Acid Metabolism in Collagen Synthesis," (in English), *Frontiers in Oncology*, Review vol. Volume 11 - 2021, 2021.

https://doi.org/10.3389/fonc.2021.719922.

[37] L. Zhang *et al.*, "Recent Progress on Structure Manipulation of Poly(vinylidene fluoride)-Based Ferroelectric Polymers for Enhanced Piezoelectricity and Applications," *Advanced Functional Materials*, vol. 33, no. 38, p. 2301302, 2023.

https://doi.org/10.1002/adfm.202301302.

[38] W. Zhang, Z. Zhang, M. Li, and X. Chen, "GPU implementation of curved-grid finite-difference modelling for non-planar rupture dynamics," *Geophysical Journal International*, vol. 222, no. 3, p. 2121-2135, 2020.

https://doi.org/10.1093/gji/ggaa290.

[39] M.-F. Marqa, P. Colin, P. Nevoux, S. R. Mordon, and N. Betrouni, "Focal Laser Ablation of Prostate Cancer: Numerical Simulation of Temperature and Damage Distribution," *BioMedical Engineering OnLine*, vol. 10, no. 1, p. 45, 2011.

https://doi.org/10.1186/1475-925X-10-45.

[40] J. A. Grant, M. A. Gallardo, and B. T. Pickup, "A fast method of molecular shape comparison: A simple application of a Gaussian description of molecular shape," *Journal of Computational Chemistry*, vol. 17, no. 14, p. 1653-1666, 1996.

https://doi.org/10.1002/(SICI)1096-987X(19961115)17:14%3C1653::AID-JCC7%3E3.0.CO;2-K.

[41] S. Altürk, D. Avcı, Ö. Tamer, and Y. Atalay, "Comparison of different hybrid DFT methods on structural, spectroscopic, electronic and NLO parameters for a potential NLO material," *Computational and Theoretical Chemistry*, vol. 1100, p. 34-45, 2017.

https://doi.org/10.1016/j.comptc.2016.12.007.

[42] G. Gao, X. Sun, and G. Liang, "Nanoagent-Promoted Mild-Temperature Photothermal Therapy for Cancer Treatment," *Advanced Functional Materials*, vol. 31, no. 25, p. 2100738, 2021.

https://doi.org/10.1002/adfm.202100738.

[43] Y. C. Shin, B. Wu, S. Lei, G. J. Cheng, and Y. Lawrence Yao, "Overview of Laser Applications in Manufacturing and Materials Processing in Recent Years," *Journal of Manufacturing Science and Engineering*, vol. 142, no. 11, 2020.

https://doi.org/10.1115/1.4048397.

[44] N. C. Giglio *et al.*, "Rapid sealing and cutting of porcine blood vessels, ex vivo, using a high-power, 1470-nm diode laser," *Journal of biomedical optics*, vol. 19, no. 3, p. 038002-038002, 2014.

https://doi.org/10.1117/1.JBO.19.3.038002.

[45] S. Singh and R. Repaka, "Temperature-controlled radiofrequency ablation of different tissues using two-

compartment models," *International Journal of Hyperthermia*, vol. 33, no. 2, p. 122-134, 2017. https://doi.org/10.1080/02656736.2016.1223890.

[46] N. I. Platnick and D. E. Rosen, "Popper and Evolutionary Novelties," *History and Philosophy of the Life Sciences*, vol. 9, no. 1, p. 5-16, 1987. http://www.jstor.org/stable/23328766.

[47] Q. Yang *et al.*, "A diamond made microchannel heat sink for high-density heat flux dissipation," *Applied Thermal Engineering*, vol. 158, p. 113804, 2019. https://doi.org/10.1016/j.applthermaleng.2019.113804.

[48] V. Oswal, M. Remacle, S. Jovanovic, S. M. Zeitels, J. P. Krespi, and C. Hopper, "Principles and Practice of Lasers in Otorhinolaryngology and Head and Neck Surgery," *The Journal of Laryngology & Otology*, vol. 128, no. 6, p. 571-572, 2014. https://doi.org/10.1017/S0022215114001194.